Redox Biology 28 (2020) 101336

Contents lists available at ScienceDirect

Redox Biology

journal homepage: www.elsevier.com/locate/redox

Research Paper

Inhibiting microRNA-144 potentiates Nrf2-dependent antioxidant signaling in RPE and protects against oxidative stress-induced outer retinal degeneration

Ravirajsinh N. Jadeja[a,*], Malita A. Jones[a], Ammar A. Abdelrahman[a,b], Folami L. Powell[a], Menaka C. Thounaojam[c], Diana Gutsaeva[c], Manuela Bartoli[c,d], Pamela M. Martin[a,c,d,e,**]

[a] Departments of Biochemistry and Molecular Biology, Medical College of Georgia at Augusta University, Augusta, GA, 30912, USA
[b] Department of Clinical Pharmacy, Faculty of Pharmacy, Cairo University, Cairo, 11562, Egypt
[c] Departments of Ophthalmology, Medical College of Georgia at Augusta University, Augusta, GA, 30912, USA
[d] Department of Culver Vision Discovery Institute and Medical College of Georgia at Augusta University, Augusta, GA, 30912, USA
[e] Georgia Cancer Center, Medical College of Georgia at Augusta University, Augusta, GA, 30912, USA

ARTICLE INFO

Keywords:
Nrf2
Oxidative stress
microRNA
miR-144
Retinal pigment epithelium
RPE

ABSTRACT

The retinal pigment epithelium (RPE) is consistently exposed to high levels of pro-oxidant and inflammatory stimuli. As such, under normal conditions the antioxidant machinery in the RPE cell is one of the most efficient in the entire body. However, antioxidant defense mechanisms are often impacted negatively by the process of aging and/or degenerative disease leaving RPE susceptible to damage which contributes to retinal dysfunction. Thus, understanding better the mechanisms governing antioxidant responses in RPE is critically important. Here, we evaluated the role of the redox sensitive microRNA miR-144 in regulation of antioxidant signaling in human and mouse RPE. In cultured human RPE, miR-144-3p and miR-144-5p expression was upregulated in response to pro-oxidant stimuli. Likewise, overexpression of miR-144-3p and -5p using targeted miR mimics was associated with reduced expression of Nrf2 and downstream antioxidant target genes (NQO1 and GCLC), reduced levels of glutathione and increased RPE cell death. Alternately, some protection was conferred against the above when miR-144-3p and miR-144-5p expression was suppressed using antagomirs. Expression analyses revealed a higher conservation of miR-144-3p expression across species and additionally, the presence of two potential Nrf2 binding sites in the 3p sequence compared to only one in the 5p sequence. Thus, we evaluated the impact of miR-144-3p expression in the retinas of mice in which a robust pro-oxidant environment was generated using sodium iodate (SI). Subretinal injection of miR-144-3p antagomir in SI mice preserved retinal integrity and function, decreased oxidative stress, limited apoptosis and enhanced antioxidant gene expression. Collectively, the present work establishes miR-144 as a potential target for preventing and treating degenerative retinal diseases in which oxidative stress is paramount and RPE is prominently affected (e.g., age-related macular degeneration and diabetic retinopathy).

1. Introduction

The retinal pigment epithelium (RPE), a single layer of polarized cuboidal epithelial cells lining the posterior segment of the eye, is situated between the photoreceptor cells and the choriocapillaris [1,2]. Congruent with its location, RPE performs many functions essential to retinal health and function. Similar to the endothelium of the inner retina, RPE forms a blood-retinal barrier in the outer retina that regulates the uptake of ions, water, and nutrients and the removal of metabolic waste products from the subretinal space to maintain metabolic homeostasis and nourishment of the photoreceptor cells [1,2]. Additionally, RPE maintains photoreceptor outer segment length; phagocytosing shed segments daily and, is involved in retinoid storage and metabolism [1,2].

Congruent with the numerous essential functions performed by RPE, this epithelial layer has a considerably high energy demand. This demand is met by the robust metabolic activity of the enriched mitochondrial population within this cell type. In turn however, a high

* Corresponding author.
** Corresponding author. Departments of Biochemistry and Molecular Biology, Medical College of Georgia at Augusta University, Augusta, GA, 30912, USA.
E-mail addresses: rjadeja@augusta.edu (R.N. Jadeja), pmmartin@augusta.edu (P.M. Martin).

https://doi.org/10.1016/j.redox.2019.101336
Received 27 July 2019; Received in revised form 11 September 2019; Accepted 26 September 2019
Available online 29 September 2019

amount of reactive oxygen species (ROS) is generated [3,4]. ROS production in RPE is further exacerbated by the immense influx of light and very high levels of oxygen that this epithelial layer is exposed to on a regular basis [4,5]. Therefore, given the high amount of ROS generated within RPE, it is not surprising that endogenous antioxidant defense mechanisms within this cell type are robust. In fact, under normal conditions, cellular levels of reduced glutathione, the most abundant endogenous antioxidant in the body, are extremely high in RPE. With advancing age and/or the onset and progression of degenerative disease however, plasma levels of glutathione and related glutathione-synthesizing enzymes decrease as does the overall efficiency with which RPE performs many of its functions [6,7]. Irrespective of whether these phenomena occur dependently or independently, a subject that is met with some debate, they indisputably contribute collectively to the accumulation of waste products within and below RPE and, the potentiation of a cellular environment conducive to the interaction of unquelled free radicals with DNA, proteins and lipids. These events propel a viscous cycle that magnifies oxidative stress, inflammation and consequent cellular dysfunction [8–10].

Given the major detriment to RPE health and function imposed by excessive pro-oxidant exposure and the related potential impact on overall retinal health and visual function [11,12] understanding better the mechanisms by which RPE amplifies antioxidant signaling and counters pro-oxidant insult under normal conditions is important, especially towards the development of novel therapeutic strategies to enhance the antioxidant capacity of these cells and preserve them in disease. Along these lines, nuclear factor erythroid 2-related factor 2 (Nrf2), a redox-sensitive transcription factor that binds to antioxidant response elements located in the promoter region of genes encoding many antioxidant enzymes and phase II detoxifying enzymes [13,14], has received much attention. Activation of Nrf2 and downstream target genes is thought to be one of the most critical defensive mechanisms against oxidative stress in many species. In keeping with this, a number of Nrf2-inducing agents have been brought forth as potential therapeutic candidates to treat degenerative retinal disease (e.g., sulforaphane, monomethylfumarate) [15–18]. These compounds provide an avenue for bolstering the expression and activity of Nrf2 and downstream antioxidant genes temporarily however, understanding better the mechanisms by which Nrf2 activity is regulated in the normal healthy RPE and how these mechanisms are impacted in aging and disease, conditions in which Nrf2 activity has been demonstrated to decline, is essential to developing effective strategies to boost endogenous antioxidant defense to protect and preserve RPE health and viability long-term [19,20].

MicroRNAs (miRNAs, miRs) are an evolutionarily conserved class of small noncoding RNAs of 22–24 nucleotides in length that act as post-transcriptional regulators of gene expression by binding to the 3'-untranslated region (3'-UTR) to induce mRNA degradation, and/or translational repression in diverse biological processes [21]. A burgeoning literature suggests that oxidative stress stimulates the production of several miRNAs known as oxidative stress-responsive miRNAs [22]. Importantly, these miRNAs have been demonstrated to play a role in connecting the dysregulated antioxidant defense system with the imbalanced redox state in a number of age- and/or disease-related cell and tissue systems [23,24]. miR-144 is one such miRNA. The potential link between miR-144 and Nrf2 signaling has been explored in a number of cells and tissue types congruent with pathology development and progression [20,25–27]. A previous study by Garcia et al., 2015 evaluated changes in miRNA expression in chronically stressed iPSC-derived RPE cells [28]. Although, this *in vitro* study reported a correlation between miR-144 and Nrf2, the specific involvement of 5p or 3p variant and the *in vivo* effects of miR-144 were not studied. In the present study, we evaluated the relevance of miR-144 to the expression of Nrf2 and downstream Nrf2 target genes in cultured human RPE and, to overall retinal health in the sodium-iodate mouse, a classic rodent model of oxidant-induced retinal degeneration [29–32].

2. Materials and methods

2.1. Cell culture

Human retinal pigment epithelial (ARPE-19) cells were cultured in Dulbecco's modified Eagle medium DMEM/F12 medium (supplemented with 10% fetal bovine serum, 100 U/ml penicillin, and 100 µg/ml streptomycin) and maintained at 37 °C in a humidified chamber with 5% CO_2. The culture medium was replaced with fresh medium every other day. Cultures were passaged by dissociation in 0.05% (w/v) trypsin in phosphate-buffered saline. Only confluent, well-differentiated RPE cultures were used for experimentation.

2.2. miRNA transfection studies

ARPE-19 cells were transfected with 50 or 100 nM miR-144-3p or miR144-5p inhibitor and/or mimic using Hiperfect Transfection Reagent (Qiagen, USA). Cells were incubated at 37 °C, 5% CO_2 for 48 h prior to collection for experimental assays. For each experiment, control cells were transfected with scrambled miRNA.

2.3. Reverse transcription–quantitative polymerase chain reaction

Total miRNA and RNA was isolated from RPE/eyecup of mice or from cultured ARPE-19 cells using miRNAeasy mini and RNAeasy kits, respectively (Qiagen, USA). cDNA was prepared from total miRNA and RNA using the miScript RT (Qiagen, USA) and iScript cDNA synthesis (Bio-Rad) kits, respectively, and was subjected to qPCR assay. mRNA qPCR assays were performed in 96-well PCR plates using All-in-One™ qPCR Mix (Genecopia, USA). The reaction volume of 20 µl for mRNA analysis contained 10 µl SYBR green master mix (2X), 1 µl cDNA, 1 µl of each primer and 7 µl nuclease-free water. Primer sequences are listed in Table S1. The following two-step thermal cycling profile was used (StepOnePlus Real-Time PCR, Life Technologies, Grand Island, NY): Step I (cycling): 95 °C for 5 min, 95 °C for 15 s, 60 °C for 30 s and 72 °C for 15s for 40 cycles. Step II (melting curve): 60 °C for 15 s, 60 °C 1 min and 95 °C for 30 s. The template amplification was confirmed by melting curve analysis. mRNA expression of genes was normalized to 18s ribosomal RNA expression and the fold change in expression was calculated by $2^{-\Delta\Delta Ct}$ method.

The reaction volume of 20 µl for miRNA analysis contained 10 µl Quantitact SYBR green master mix (2X), 2 µl cDNA, 2 µl of universal primer, 2 µl of miRNA specific primer and 4 µl nuclease-free water. miRNA primer sequences are listed in Table S2. The following two-step thermal cycling profile was used (StepOnePlus Real-Time PCR, Life Technologies, Grand Island, NY): Step I (cycling): 95 °C for 15 min, 94 °C for 15 s, 55 °C for 30 s and 70 °C for 30s for 40 cycles. Step II (melting curve): 60 °C for 15 s, 60 °C 1 min and 95 °C for 30 s. The template amplification was confirmed by melting curve analysis. miRNA expression of genes was normalized to 5s expression and fold change in expression was calculated by the $2^{-\Delta\Delta Ct}$ method.

2.4. Western blotting

Total protein was extracted from RPE/eyecup of mice or from human RPE (ARPE-19) cells using RIPA cell lysis buffer (Thermo Scientific, USA) containing protease and phosphatase inhibitors and concentration was determined using the Coomassie protein assay reagent (Sigma-Aldrich, USA). Equivalent amount of protein samples (40–60 µg) were subjected to SDS–PAGE, transferred onto PVDF membranes, and then incubated with primary antibodies: Nrf2 (1:250, cell signaling), GCLC, HO-1 (1:1000, Abcam, USA), NQO1 (1:1000, Santa cruz biotech, USA) overnight at 4 °C. Next day, blots were washed with TBST (tris buffered saline with tween 20) and incubated with horseradish peroxidase conjugated secondary antibody (1:3000; Sigma-Aldrich, USA) for 60 min with gentle shaking at room temperature.

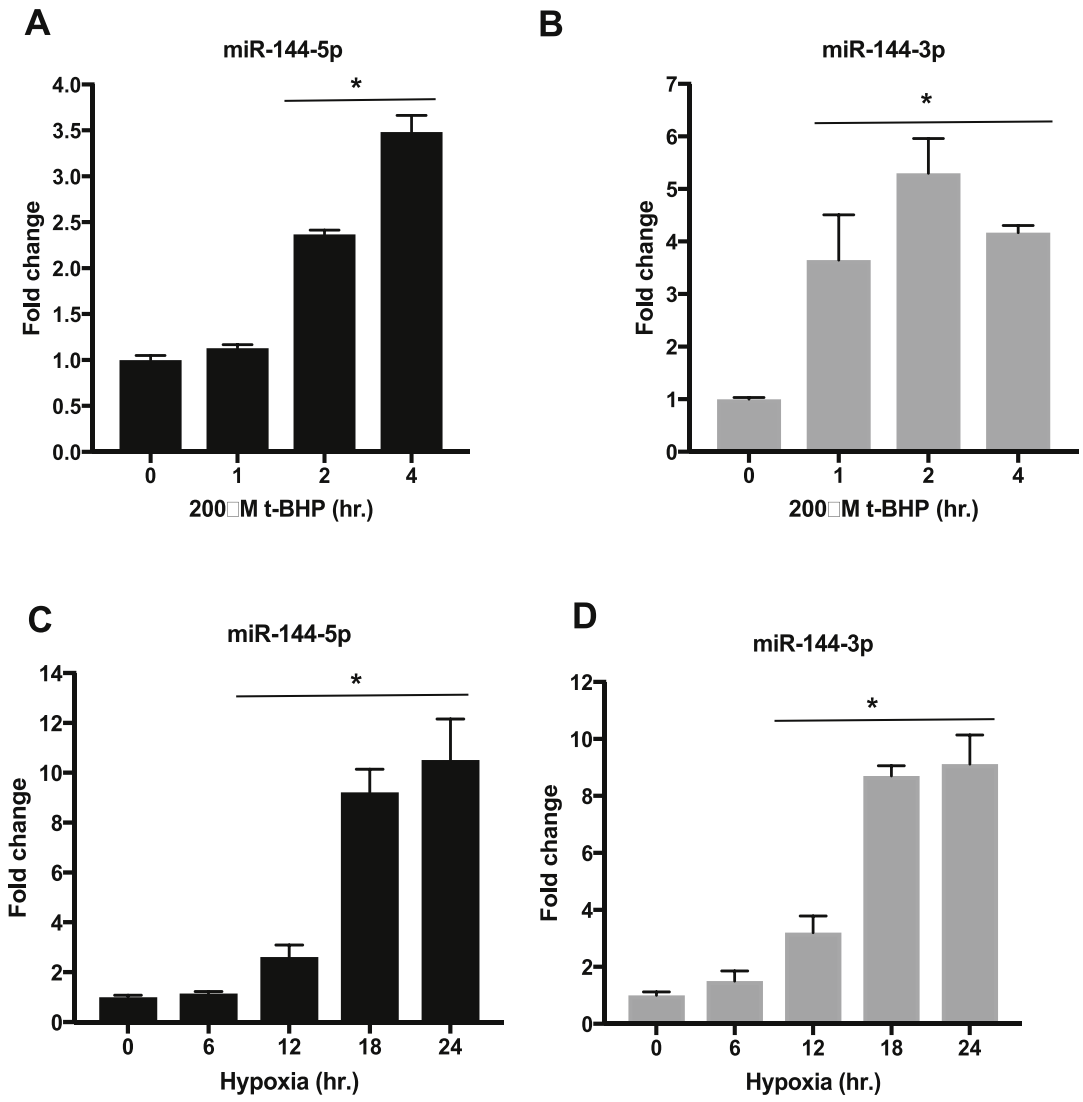

Fig. 1. Oxidative stress up regulates miR-144 expression in cultured human retinal pigment epithelial cells.
(A–B) Human retinal pigment epithelial (ARPE-19) cells were treated with 200 μM tert-butyl hydroperoxide (t-BHP) for 1, 2, and 4 h miR-144-5p and miR-144-3p expression was then evaluated by qPCR assay. **(C–D)** ARPE-19 cells were cultured in hypoxic conditions (2% oxygen) for 6, 12, 18 and 24 h and, miR-144-5p and miR-144-3p expression was evaluated by qPCR assay. Results are expressed as mean ± S.E.M for n = 3 independent experiments. *$p < 0.05$ vs. untreated cells (0 h).

Blots were then washed with TBST and developed with chemiluminescence reagent (Bio-Rad, Hercules, CA) using autoradiography films (Genesee Scientific, San Diego, CA). β-actin (1:3000; Sigma-Aldrich, USA) expression was evaluated to determine equivalent loading. Scanned images of blots were used to quantify protein expression using NIH ImageJ software (http://rsb.info.nih.gov/ij/) and expressed as fold change.

2.5. 3′-UTR binding luciferase assay

For luciferase reporter analyses, the 3′-UTR of the human Nrf2 gene amplified by PCR from human cDNA was cloned into the pEZX-MT05 (GeneCopoeia, Rockville, MD). ARPE-19 cells were seeded into 96-well plates and transfected using Hiperfect tranfection reagent as described above. Cells were co-transfected with 100 nM miR-144-3p mimic, miR-144-5p mimic, or negative control (NC) miRNA oligonucleotide duplexes and 1 μg of pEZX-MT05 with or without the 3′-UTR of the human Nrf2 gene. After 24 h, culture media was refreshed and at 48 h, activities of Gaussia luciferase (GLuc) and secreted alkaline phosphatase (SEAP) were determined with a luminometer. The relative reporter activity was obtained by normalizing the GLuc activity against SEAP activity.

2.6. CellROX assay

ARPE-19 cells were treated with 200 μM tert-butyl hydroperoxide (t-BHP) for different time intervals to induce oxidative stress. At the end of treatments, cells were incubated with 5 μM CellROX for 30 min, washed with PBS (phosphate buffered saline) and mounted using fluoroshield mounting medium with DAPI (Sigma Aldrich, St. Louis, MO). The images were captured at 20X magnification using Zeiss Axioplan-2 imaging fluorescence microscope (Carl Zeiss, Göttingen, Germany).

2.7. MTT cell viability and LDH cytotoxicity assays

ARPE-19 cells were transfected with scramble non-targeted control, miR-144-5p or miR-144-3p mimic or inhibitor (antagomiR) and treated with 200 μM t-BHP. After different time intervals (0–4 h), culture media was replaced with 100 μl MTT (Sigma-Aldrich, St. Louis, MO) solution (0.5 mg/ml in culture media) and incubated at 37 °C. After 3 h, MTT solution was discarded; all wells were washed with PBS and 100 μl

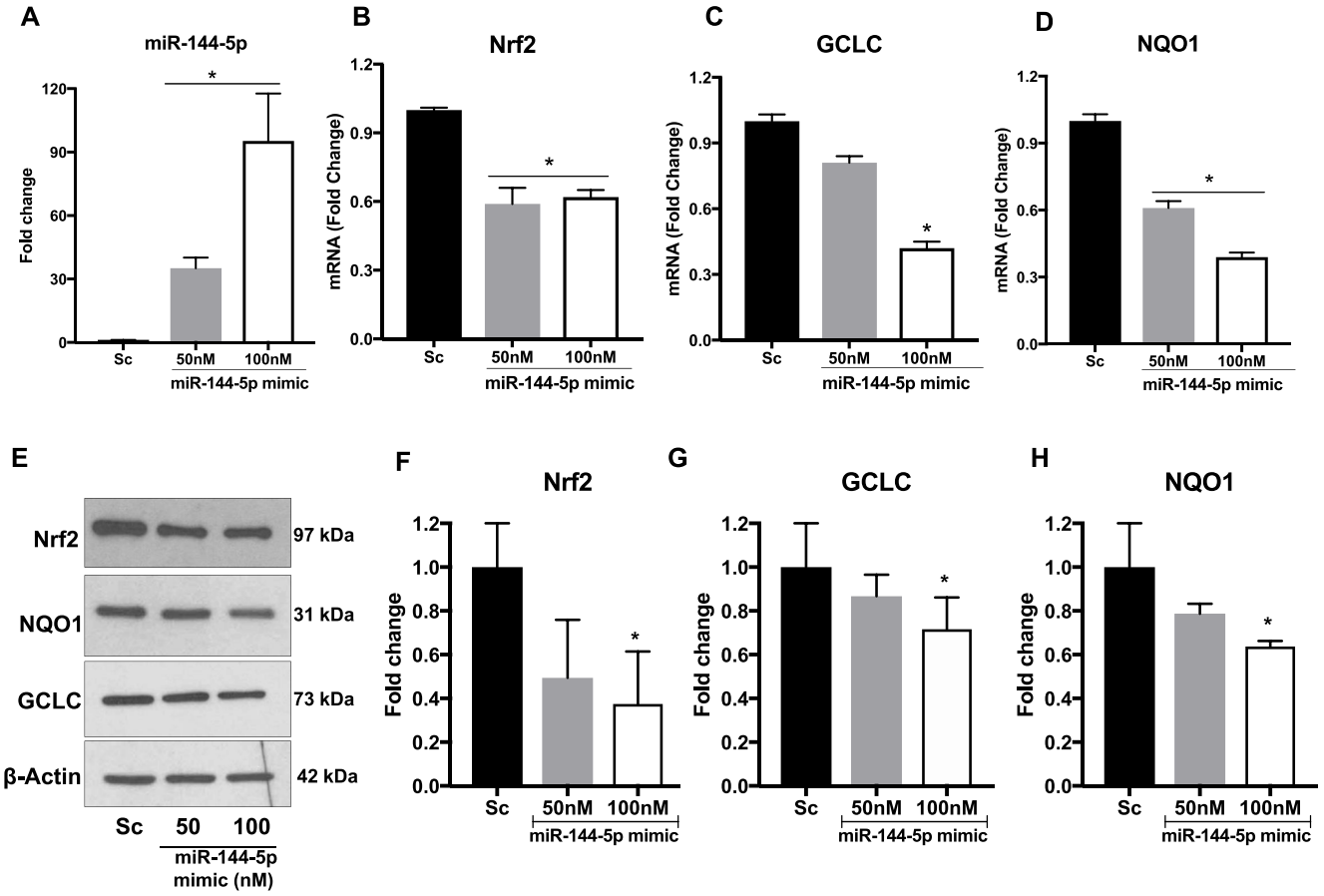

Fig. 2. miR-144-5p regulates Nrf2 expression in cultured human retinal pigment epithelial cells.
(A) miR-144-5p was overexpressed in human retinal pigment epithelial (ARPE-19) cells by transfecting cells with 50 or 100 nM miR-144-5p mimic for 48 h. The efficacy of miR-144-5p overexpression using varying doses of miR-144-5p mimic was then evaluated by qPCR. Protein and RNA were additionally extracted such that **(B–D)** mRNA and **(E–H)** protein levels of Nrf2, GCLC and NQO1 could be evaluated by qPCR and Western blotting, respectively. (E) A representative Western blot image from three replicates is shown. All graphical results are expressed as mean ± S.E.M for three independent experiments. *$p < 0.05$ vs. scramble miRNA (Sc) transfected cells. Nrf2: Nuclear factor erythroid 2–related factor 2; GCLC: Glutamate-cysteine ligase catalytic subunit; NQO1: NAD(P)H Quinone Dehydrogenase 1.

DMSO was added to each well. The absorbance was read at 540 nm (VersaMax Microplate Reader, Molecular Device, Sunnyvale, CA) and data was expressed as percent cell viability.

The amount of lactate dehydrogenase (LDH) released in the cell culture media was assessed using Pierce LDH Cytotoxicity assay kit as per manufacturer's instruction (Thermo Scientific, Wilmington, DE). In 96-well plates, ARPE19 cells were treated as mentioned above. At the end of incubation, 50 µl cell culture media from the different wells was mixed with 50 µl reaction mixture and incubated in dark at room temperature. After 30 min, 50 µl stop solution was added and absorbance was read at 490 and 680 nm on a VersaMax Microplate Reader (Molecular Device, Sunnyvale, CA). LDH release is presented as percent cytotoxicity, which was calculated per the manufacturer's instruction.

2.8. Animals

All experiments involving animals adhered to the Public Health Service Policy on the Humane Care and Use of Laboratory Animals (2015 Department of Health, Education and Welfare publication, NIH 80-23), the Association for Research in Vision and Ophthalmology Statement for use of Animals in Ophthalmic and Vision Research and were approved by the Augusta University Institutional Animal Care and Use Committee. Eight-week-old male C57BL/6J mice obtained from a commercial vendor (Jackson Laboratories, Bar Harbor, ME, USA) were housed under identical conditions in a pathogen-free environment with a 12:12 h light/dark cycle and free access to laboratory chow and water. Mice were acclimatized to the housing environment for at least 1 week before the experiments.

2.9. Sodium iodate induced-RPE injury model

The mouse model of sodium iodate-induced retinal degeneration, an established and widely used model of pro-oxidant induced outer retinal damage, was developed as per the protocol of Chowers et al., 2017 [29]. Just prior to injection, sodium iodate ($NaIO_3$; Sigma-Aldrich Corp., St. Louis, MO, USA) was dissolved in saline (0.9% sterile sodium chloride). Eight-week-old male C57BL/6J mice then received a single intraperitoneal injection of 50 mg/kg $NaIO_3$. One set of $NaIO_3$ treated mice were injected sub-retinally with 5 µg miR-144-3p inhibitor (anti-miR-144-3p) on day 2. As an internal control, the contralateral eye of these mice received a single subretinal injection of scrambled miRNA. Both eyes of mice in the vehicle group received a single subretinal injection of saline. At the end of 14 days all mice were sacrificed and the eyes collected for miRNA, RNA, protein and histopathologic analyses.

2.10. Histopathology

Eyes were fixed in 4% paraformaldehyde and cryopreserved. Serial sections (5 um thickness) were prepared and stained with hematoxylin and eosin (H&E) such that morphologic analyses of central, temporal and nasal regions of retina (relative to the optic nerve) could be performed.

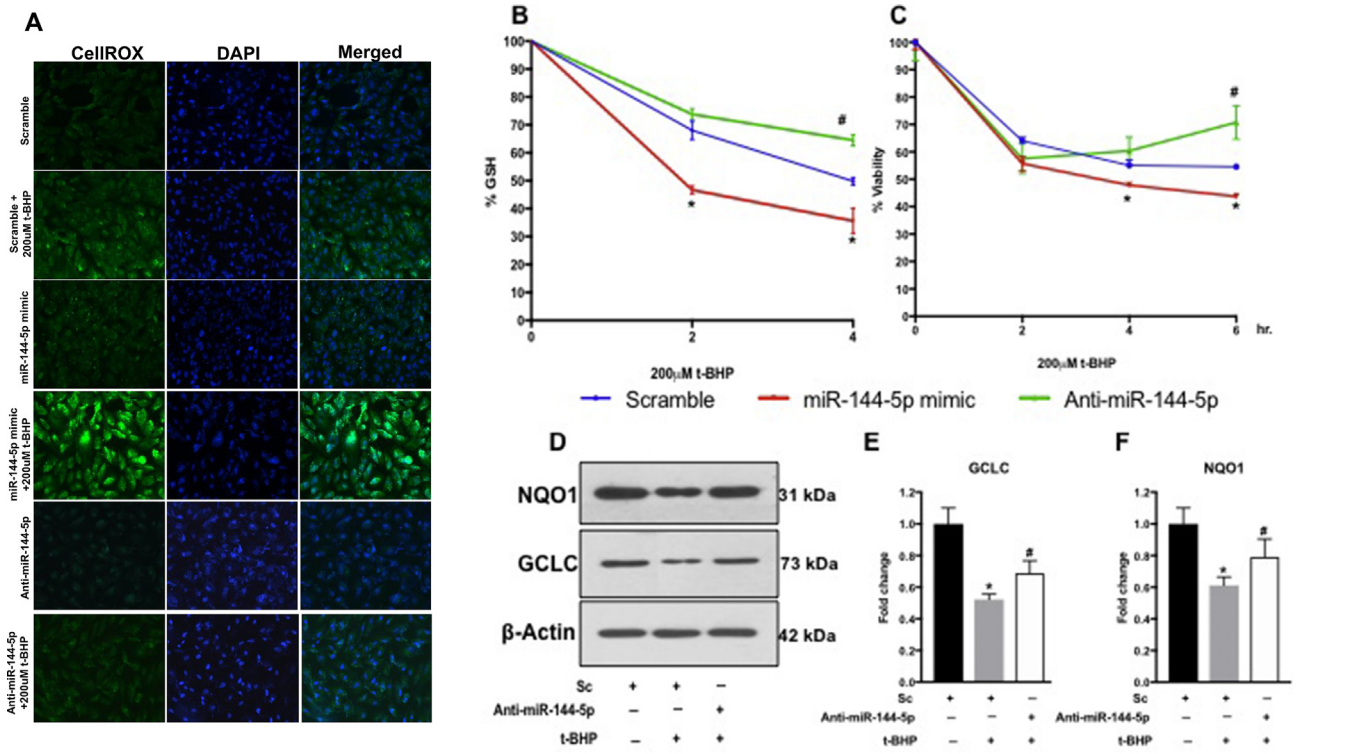

Fig. 3. miR-144-5p regulates antioxidant signaling in cultured human retinal pigment epithelial cells.
miR-144-5p overexpression or inhibition was achieved by transfecting human retinal pigment epithelial cells (ARPE-19) with 100 nM miR144-5p mimic or antagomir, respectively, for 48 h. To induce oxidative stress, cultures were exposed to 200 μM t-BHP (tert-Butyl hydroperoxide) for different time intervals. **(A)** CellROX staining was used to evaluate levels of oxidative stress in cultures after 2 h treatment. **(B)** GSH levels and **(C)** cell viability (MTT assay) were also monitored across the different treatment conditions and timepoints. **(D–F)** Western blotting was used to evaluate antioxidant enzyme protein expression. **(D)** A representative Western blot image from three replicates is shown. Results are expressed as mean ± S.E.M for three independent experiments. *$p < 0.05$ vs. scramble miRNA (Sc) transfected cells. GSH: Reduced glutathione; Nrf2: Nuclear factor erythroid 2–related factor 2; GCLC: Glutamate-cysteine ligase catalytic subunit; NQO1: NAD(P)H Quinone Dehydrogenase 1.

Three different retina locations within a 500 μm radius of the optic nerve in each eye were used to measure the lengths of the inner and outer segments (IS, OS) and to count nuclei of the photoreceptors. Additionally, the thickness of the inner nuclear layer (INL), outer nuclear layer (ONL) and nerve fiber layer (NFL) was measured and, the number of overt disruptions (bumps or breaks) in the organization of the RPE layer were calculated in a 200 μm length of retina which was randomly chosen from each of the three different locations mentioned above.

2.11. TUNEL assay

DNA fragmentation, an indication of apoptosis, was monitored in frozen retinal sections by terminal deoxynucleotidyl transferase dUTP nick end labeling (TUNEL) assay (DeadEnd Fluorimetric TUNEL System, Promega, Madison, WI) per the manufacturer's instructions. In brief, the assay detects fragmented DNA in cells by catalytically incorporating fluorescein-12-dUTP at the 3'-OH DNA ends using the enzyme terminal deoxynucleotidyl transferase (TdT). Images were obtained using a Zeiss Axioplan 2 fluorescent imaging microscope (Carl Zeiss Inc. Germany) at 20X magnification.

2.12. Immunofluorescence staining

Retinal cryosections were incubated overnight at 4 °C with anti-mouse 4-hydroxynonenal (4-HNE) antibody (1:100; Cayman Chemical, Ann Arbor, Michigan). Slides were washed three times with 0.1% Triton X-100 in 0.1 M PBS (pH 7.4) followed by a 1 h incubation with goat anti-rabbit IgG-conjugated Alexa flour 488 secondary antibody (Molecular probes-Life Technologies, Grand Island, NY). Coverslips were mounted using fluoroshield mounting medium with DAPI (Sigma-Aldrich, St. Louis, MO) and images captured at 20X magnification using Zeiss Axioplan-2 imaging fluorescence microscope (Carl Zeiss, Göttingen, Germany).

2.13. Dihydroethidium staining for detection of superoxide

Retinal cryosections were brought to room temperature and subsequently covered with 10 μM dihydroethidium (DHE) solution. Slides were incubated in a light-protected humidified incubator at 37 °C for 30 min. At the end of the incubation, sections were mounted with a coverslip and images were captured at 20X magnification using Zeiss Axioplan-2 imaging fluorescence microscope (Carl Zeiss, Göttingen, Germany).

2.14. Optokinetic tracking (OKT) response

Optokinetic testing (OptoMotry; Cerebral Mechanics, Inc., Lethbridge, AB, Canada) was performed to monitor visual acuity was monitored in mice as described previously [33]. In brief, mice were placed one at a time on a small platform in the center of four computer monitors. The optokinetic reflex to a rotating visual stimulus displayed on four LCD panels surrounding the mouse that formed a virtual drum with a rotating vertical sine wave grating (12°/s (d/s)) was then recorded by tracking response. Reflexive head movements in the same direction as the rotating gratings were considered positive responses. Spatial frequency thresholds were determined with an increasing staircase paradigm starting at 0.042 cycles/deg (c/d) with 100%

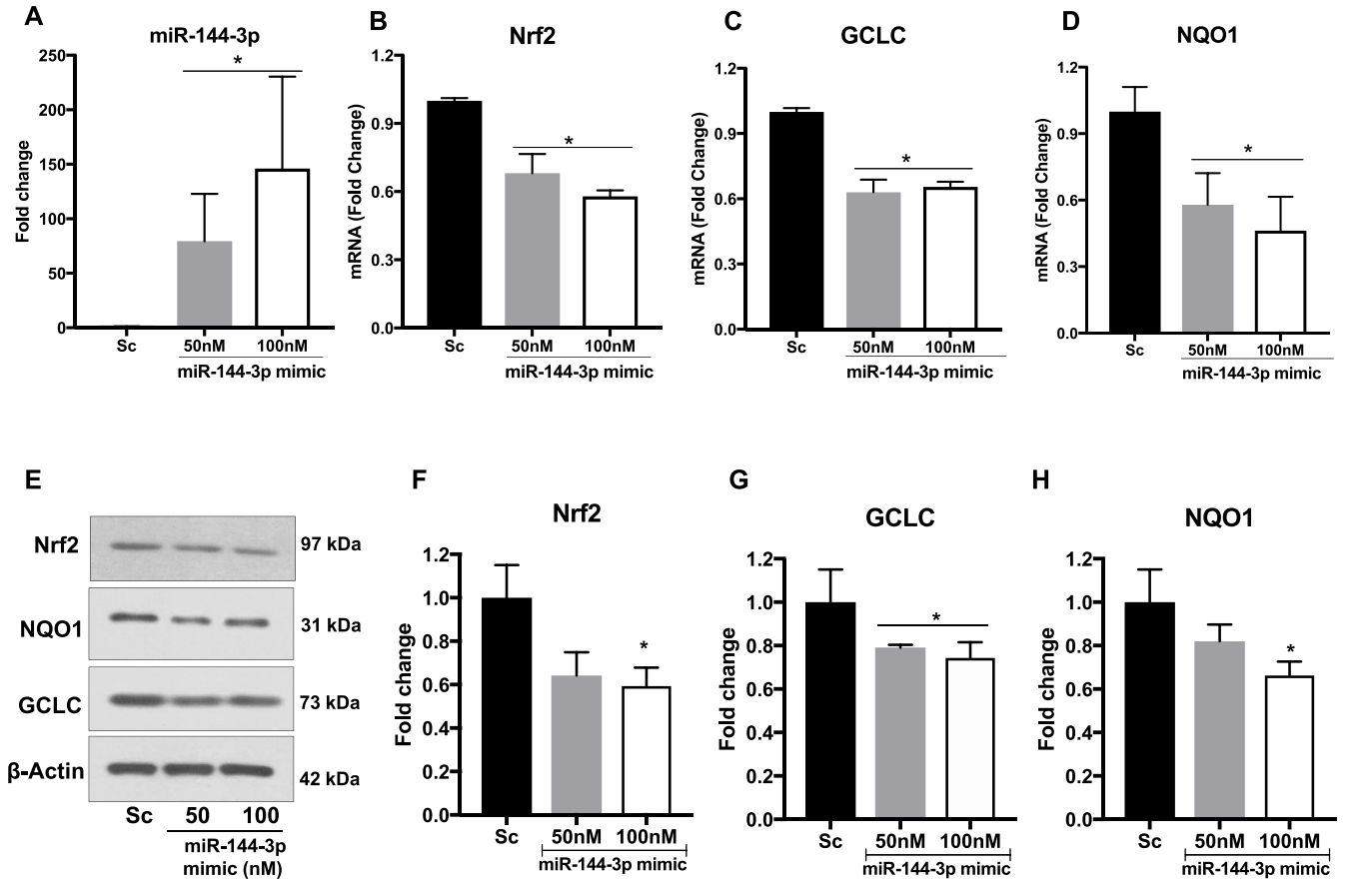

Fig. 4. miR-144-3p regulates Nrf2 expression in cultured human retinal pigment epithelial cells.
(A) miR-144-3p was overexpressed in human retinal pigment epithelial (ARPE-19) cells by transfecting cells with 50 or 100 nM miR-144-3p mimic for 48 h. The efficacy of miR-144-3p overexpression using varying doses of miR-144-3p mimic was then evaluated by qPCR. Protein and RNA were additionally extracted such that **(B–D)** mRNA and **(E–H)** protein levels of Nrf2, GCLC and NQO1 could be evaluated by qPCR and Western blotting, respectively. **(E)** A representative Western blot image from three replicates is shown. All graphical results are expressed as mean ± S.E.M for three independent experiments. *$p < 0.05$ vs. scramble miRNA (Sc) transfected cells. Nrf2: Nuclear factor erythroid 2–related factor 2; GCLC: Glutamate-cysteine ligase catalytic subunit; NQO1: NAD(P)H Quinone Dehydrogenase 1.

contrast.

2.15. Statistical analysis

All results are presented as mean ± S.E.M for a minimum of three independent experiments. Statistical significance was defined as $p < 0.05$ and determined using student's t-test (normally-distributed data) for single comparisons and ANOVA coupled with Tukey-Kramer post-hoc statistical tests for multiple comparisons. Graphs were prepared using GraphPad Prism 7 software.

3. Results

3.1. Oxidative stress upregulates miR-144-3p and miR-144-5p in retinal pigment epithelial cells

MicroRNA-144 (miR-144) has been identified as a stress responsive miR. Because the relevance of this miR to antioxidant signaling in RPE, a tissue exposed continually to high amounts of pro-oxidant stress, has not been evaluated, we first evaluated miR-144-3p and miR-144-5p expression in human RPE cells exposed to tert-butyl-hydroperoxide (t-BHP, 200 μM) or hypoxia (2% oxygen), experimental conditions that generate substantial oxidative stress. Both miR strands, 5p and 3p (Fig. 1A and C and, 1B and 1D, respectively), responded similarly to increasing durations of exposure to t-BHP or hypoxia. Extended exposure to t-BHP (Fig. 1A-B) or hypoxia (Fig. 1C-D) significantly upregulated RPE-specific expression of both miR-144-5p and miR-144-3p. These data not only confirm the expression of miR-144 in human RPE cells but further, support the hypothesis that in this cell type both the 5p and 3p strands of this miR function in a stress-dependent manner.

3.2. miR-144-5p regulates Nrf2 expression and antioxidant signaling in human retinal pigment epithelial cells

To evaluate the contribution of miR-144-5p and -3p in the regulation of Nrf2-dependent antioxidant signaling in human RPE cells, we next performed overexpression studies using miR mimics specific for the two strand variants. miR-144-5p was tested first (Figs. 2–3). Two doses of miR-144-5p mimic were tested, 50 nm and 100 nm. Both doses increased miR-144-5p expression significantly compared to non-targeted (scrambled, Sc) control cells though the higher dose was comparatively more effective than the lower (Fig. 2A). Further, Nrf2 expression was significantly decreased at the mRNA and protein level in association with miR-144-5p overexpression (Fig. 2B and 2E-F, respectively). To determine whether the observed alterations in Nrf2 expression translate to suppression of Nrf2 signaling, we monitored the expression of the catalytic unit of glutamate-cysteine ligase (GCLC) and NAD(P)H dehydrogenase quinone 1 (NQO1), two well established downstream targets of Nrf2. Congruent with the decline in Nrf2 expression induced by miR-144-5p overexpression, GCLC and NQO1 mRNA and protein expression were too reduced (Figs. 2C-D and 2E, G-H, respectively).

The data obtained to this point suggest strongly that miR-144-5p inversely regulates Nrf2 expression and downstream signaling.

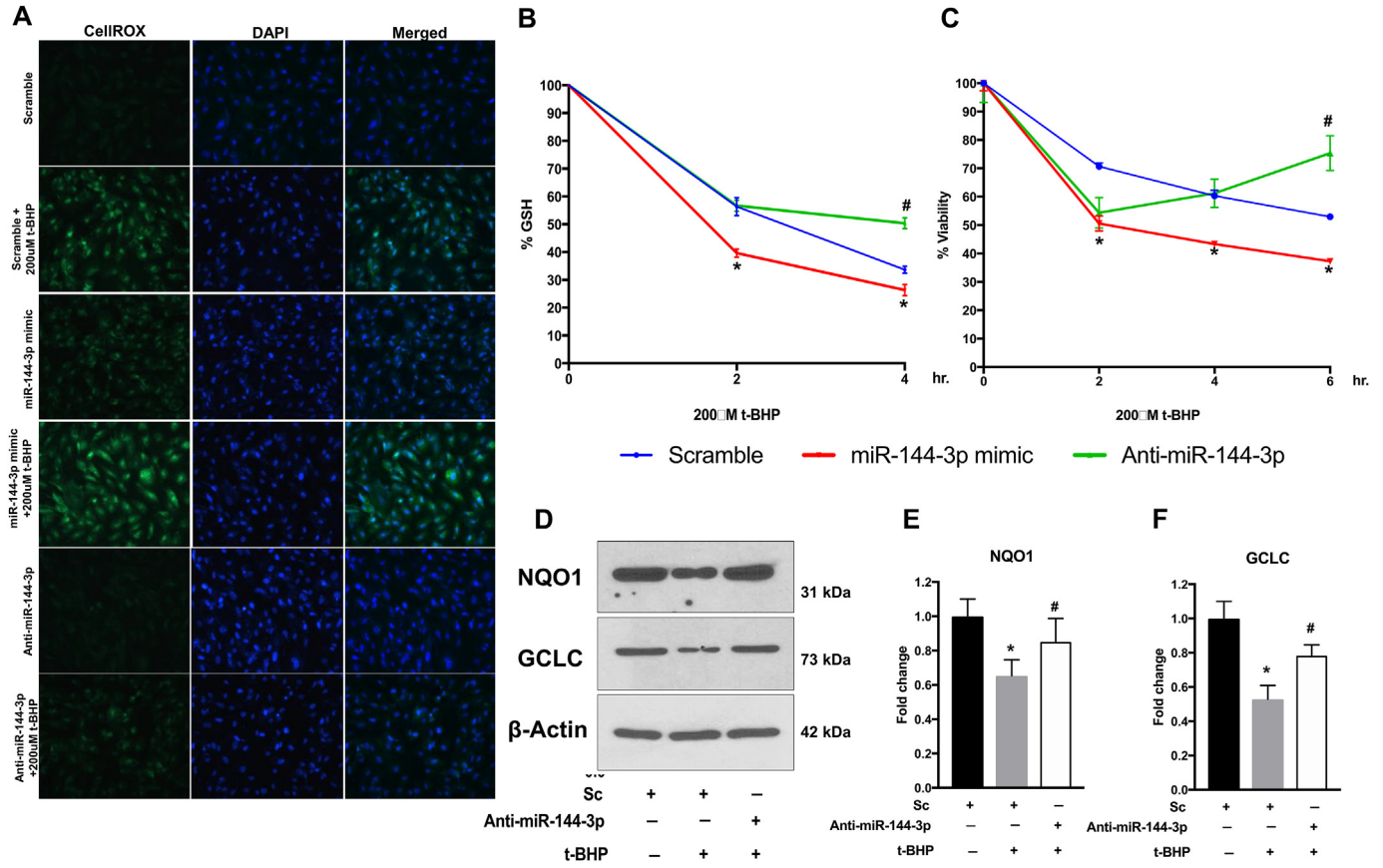

Fig. 5. miR-144-3p regulates antioxidant signaling in cultured human retinal pigment epithelial cells. miR-144-3p overexpression or inhibition was achieved by transfecting human retinal pigment epithelial cells (ARPE-19) with 100 nM miR144-3p mimic or antagomir, respectively, for 48 h. To induce oxidative stress, cultures were exposed to 200 μM t-BHP (tert-Butyl hydroperoxide) for different time intervals. **(A)** CellROX staining was used to evaluate levels of oxidative stress in cultures after 2 h treatment. **(B)** GSH levels and **(C)** cell viability (MTT assay) were also monitored across the different treatment conditions and timepoints. **(D–F)** Western blotting was used to evaluate antioxidant enzyme protein expression. **(D)** A representative Western blot image from three replicates is shown. Results are expressed as mean ± S.E.M for three independent experiments. *$p < 0.05$ vs. scramble miRNA (Sc) transfected cells. GSH: Reduced glutathione; Nrf2: Nuclear factor erythroid 2–related factor 2; GCLC: Glutamate-cysteine ligase catalytic subunit; NQO1: NAD(P)H Quinone Dehydrogenase 1.

Therefore, we predicted that under conditions of elevated miR-144-5p expression RPE would be rendered more susceptible to pro-oxidant damage. To validate this hypothesis, control and miR-144-5p-over-expressing human RPE cells were exposed to 200 μM t-BHP for 2 h. Levels of oxidative stress generated in the individual cultures were then monitored via CellROX assay, a generic ROS detection assay system (Figs. 3A). Little to no oxidative stress was detected in scrambled controls as indicated by the extremely low level of green fluorescence detected in these samples. However as expected, the intensity of green fluorescence and therefore the level of oxidative stress increased in association with t-BHP treatment. Interestingly, there was also a moderate increase in ROS generation in miR-144-5p overexpressing cells (cells transfected with miR-144-5p mimic) compared to scrambled control cells even in the absence of t-BHP exposure. ROS generation was exacerbated significantly however, when 5p-overexpressing cells were exposed to t-BHP. To confirm that the effects observed were specific to miR-144-5p overexpression, additional experiments were performed using antagomir (anti-miR-144-5p) to suppress miR-144-5p expression (Fig. S1, *A*). Nrf2 expression increased significantly in association with antagomir-mediated suppression of miR-144-5p (Fig. S1, *B*). This was reflected also in CellROX assays which confirmed that blockade of miR-144-5p expression mitigated the suppressive effects on Nrf2 as indicated by the reduced amount of oxidative stress (green fluorescence) detected in anti-miR-144-5p treated human RPE cell cultures in the presence of t-BHP (Figs. 3A). Although we used ImageJ software to quantify the relative level of fluorescence detected in images emanating from CellROX assays to confirm our visual observations (Fig. S2, *A*), the fact remains that the CellRox assay system is largely qualitative. Therefore, we additionally monitored levels of reduced glutathione (GSH, Fig. 3B) in scrambled control (blue line), miR-144-5p over-expressing (red line) and anti-miR-144-5p treated (green line) cells exposed to 200 μM t-BHP for 0–4 h. GSH levels were significantly reduced in association with miR-144-5p overexpression and alternately, were elevated significantly in association with miR-144-5p suppression by antagomir (Fig. 3B). To determine whether the effects on GSH related to differences in cell viability, MTT and lactate dehydrogenase (LDH) assays were performed (Fig. 3C; Fig. S2-*B*). Cell viability was uniformly impacted by t-BHP exposure within the first 2 h of exposure. This is reflected by the lack of significant differences in the number of viable cells in cultures transfected with scramble, miR-144-5p-mimic or miR-144-5p-antagomir at this time-point. However, notable differences in cell viability were detected across the different groups with longer durations (> 2 h) of t-BHP exposure. miR-144-5p overexpressing cells were unable to recover post 2 h exposure to t-BHP and cell viability continued to decline in these cultures with additional increases in time (Fig. 3C, red line). Scramble control cells (Fig. 3C, blue line) behaved similarly although significantly better than miR-144-5p-overexpressing cells with respect to maintenance of cell viability post-oxidant exposure. Impressively however, in cells treated with antagomir to suppress miR-144-5p expression (Fig. 3C, green line), some recovery was noted as remaining cells began to once again proliferate steadily. Collectively, these data support that the level of miR-144-5p expression

A

	Predicted consequential pairing of target region (top) and miRNA (bottom)
Position 301-313 of Nrf2 3' UTR	5' . . . AUAGAUUUAUAUGAUGAUAUAUGA . . .
hsa-miR-144-5p	3' GAAUGUCAUAUACUACUAUAGG
Position 265-271 of Nrf2 3' UTR	5' . . . UACAAAAACUUAUUUAUACUGUU . . .
hsa -miR-144-3p	3' UCAUGUAGUAGAUAUGACAU
Position 370-377 of Nrf2 3' UTR	5' . . . UGUACUUUUUUAUAAAUACUGUA . . .
hsa-miR-144-3p	3' UCAUGUAGUAGAUAUGACAU
Position 257-263 of Nrf2 3' UTR	5' . . . CUACAGAACUUAUUUAUACUGUU . . .
mmu-miR-144-3p	3' UCAUGUAGUAGAUAUGACAU
Position 349-356 of Nrf2 3' UTR	5' . . . ACUAUACUUUUUUAUAUACUGUA . . .
mmu-miR-144-3p	3' UCAUGUAGUAGAUAUGACAU

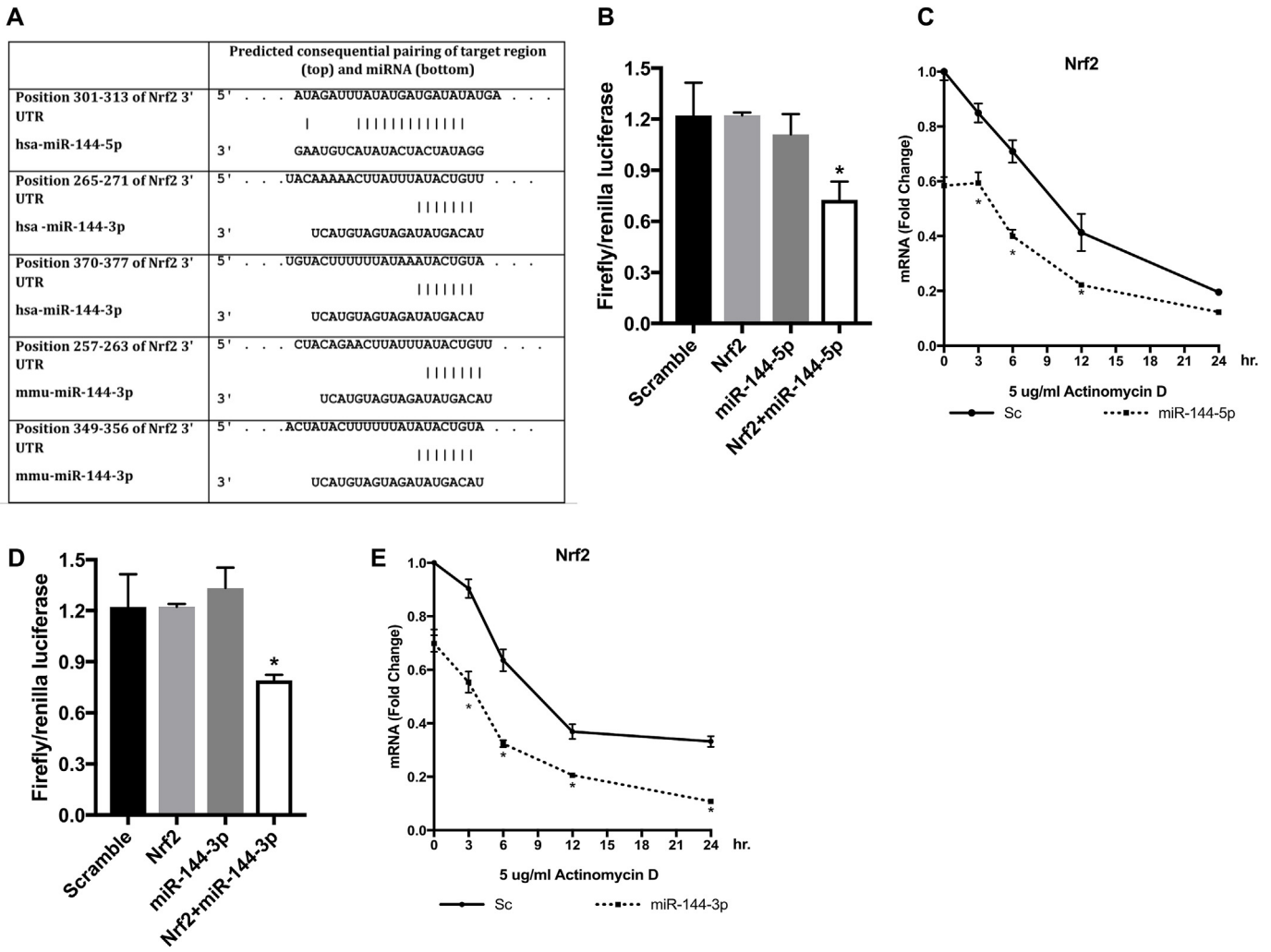

Fig. 6. miR-144-5p and 3p target the 3' UTR of Nrf2 in human retinal pigment epithelial cells.
(A) Nucleotide sequence alignment between the 3'-UTR of Nrf2 and miR-144-5p and miR-144-3p generated by targetscan (http://www.targetscan.org/vert_72/). Renilla and firefly luciferase assay was performed using Luc-Pair™ Duo-luciferase assay kit 2.0 as per the instructions of manufacturer. **(B & D)** Results of luciferase assay obtained from human retinal pigment epithelial cells (ARPE-19) transfected with miR-144-5p mimic or miR-144-3p mimic alone or in combination with plasmid containing 3'-UTR sequence for Nrf2. **(C & E)** miR-144-5p or miR-144-3p overexpressing ARPE-19 cells were treated with 5 μg/ml actinomycin D for 3, 6, 12 and 24 h to evaluated changes in Nrf2 mRNA expression by qPCR. *$p < 0.05$ vs. scramble miRNA (Sc) transfected cells.

influences directly the ability of RPE cells to effectively counter pro-oxidant stimuli. This conclusion is further supported by evaluation of GCLC and NQO1 expression at the protein level (Fig. 3D–F). GCLC and NQO1 expression was significantly reduced in control (Sc) cells in association with acute (2 h) exposure of cells to t-BHP. However, the expression of these Nrf2 target genes was bolstered significantly in association with miR-144-5p inhibition (anti-miR-144-5p) even in the presence of a pro-oxidant stimulus, t-BHP.

3.3. miR-144-3p regulates Nrf2 expression and antioxidant signaling in human retinal pigment epithelial cells

Because our initial studies (Fig. 1) revealed similarities in the pattern of miR-144-5p and miR-144-3p expression following exposure to pro-oxidant or hypoxic stimulation, studies identical to those described above (Figs. 2–3) were performed in human RPE cells except that this time miR-144-3p was overexpressed using mimic or suppressed via antagomir (Figs. 4–5). MiR-144-3p was transiently overexpressed in human RPE cells by transfecting with 50 and 100 nM miR-144-3p mimic for 48 h (Fig. 4A). As observed with miR-144-5p overexpression, Nrf2 mRNA was significantly reduced in association with overexpression of the 3p variant (Fig. 4B), as was the mRNA expression of its downstream targets GCLC and NQO1 (Figs. 4C and D, respectively). Nrf2, GCLC and NQO1 protein were similarly reduced in conjunction with increased miR-144-3p expression (Figs. 4E–H).

The impact of miR-144-3p expression on Nrf2 was further evaluated via CellROX staining of cells exposed to 200 μM t-BHP for 2h (Fig. 5A and Fig. S2-*C*). Congruent with t-BHP exposure, levels of oxidative stress were increased in control and miR-144-3p-overexpressing cells. The amount of oxidative stress generated was further enhanced by miR-144-3p overexpression as indicated by the higher intensity of green fluorescence detected cultures treated with t-BHP and miR-144-3p mimic compared to cultures treated with miR-144-3p alone. To demonstrate definitively that the results observed were dependent upon miR-144-3p expression, we inhibited miR-144-3p expression using miR-144-3p antagomir (anti-miR-144-3p; Fig. S1, *C*) and saw that doing so increased Nrf2 expression significantly (Fig. S1, *D*). Oxidative stress generation was limited in cells in association with blockade of miR-144-3p expression even in the presence of t-BHP. To better gauge the impact of miR-144-3p expression on endogenous antioxidant defense mechanisms in human RPE cells, GSH measurements were additionally obtained (Fig. 5B). Levels of GSH were reduced overall in association with t-BHP exposure. However, the ability of cells to recover from t-BHP insult correlated inversely with miR-144-3p expression. Cell

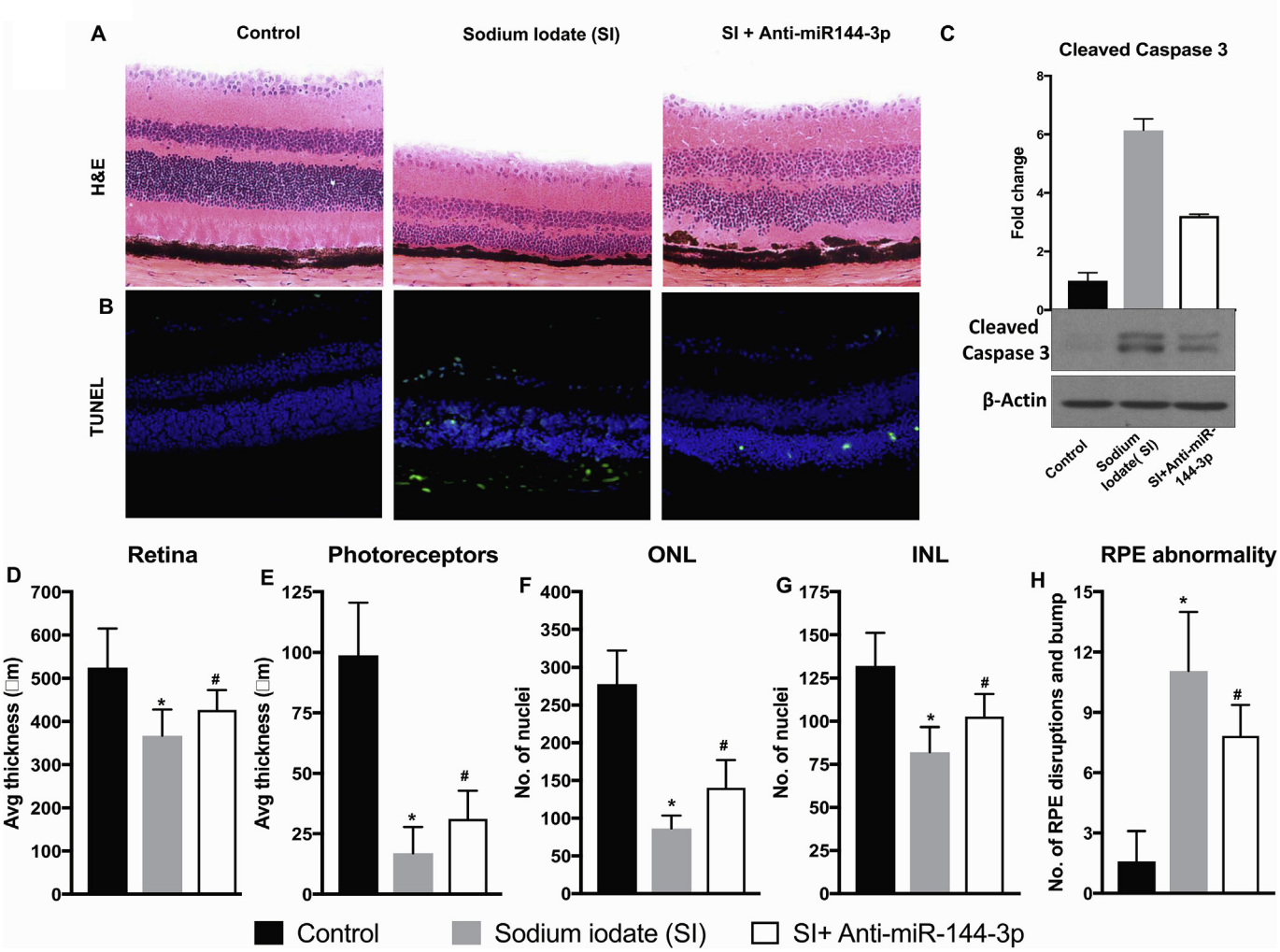

Fig. 7. Effect of miR-144-3p inhibition on sodium iodate-induced (SI) retinal degeneration in mice.
Eight weeks old male C57BL/6J mice were treated with (Control) saline (Day 0), (Sodium Iodate) 50 mg/kg SI (day 0) once and (Sodium Iodate + Anti-miR-144-3p) 50 mg/kg SI (day 0) + 5 μg anti-miR-144-3p (day 1). All animals were sacrificed on day 14 to collect RPE/eye cup for further analysis. Eyes were collected and processed for fresh frozen sectioning and **(A)** H&E and **(B)** TUNEL staining was performed. **(C)** Changes in expression of cleaved caspase-3 was evaluated by western blotting. Morphometric analyses of the thickness of the total retina **(D),** photoreceptor **(E)** and nuclear layers **(F, G)** as well as areas in which disrupted or abnormal RPE were present **(H)** was performed using Zeiss LSM Image analysis software and an investigator blinded to the study. Results are expressed as mean ± S.E.M for n = 6. *p < 0.05 vs. control mice and #p < 0.05 vs. sodium iodate.

viability and the expression of Nrf2 target genes (NQO1, GCLC) were also significantly reduced in association with elevated miR-144-3p expression (Figs. 5C–F and Fig. S2, *D*). Alternately, GSH levels, cell viability and NQO1 and GCLC expression were all significantly increased in association with miR-144-3p suppression.

3.4. miR-144-5p and 3p targets 3' UTR of Nrf2 in retinal pigment epithelial cells

The data above show clearly that both the 5p and 3p strands of miR-144 impact Nrf2 expression and downstream signaling. However, the exact mechanisms by which the regulatory effects on Nrf2 are imposed by each strand are not known. To address this, *in silico* target prediction analyses for miR-144-5p and -3p were performed (Fig. 6). The target scan report revealed that the 3'-UTR sequence of Nrf2 possesses binding sites for both miR-144-5p and miR-144-3p. Interestingly, the interaction of miR-144-3p with the 3'-UTR of Nrf2 was highly conserved through the different species whereas, miR-144-5p interacted only with the human 3'-UTR sequence of Nrf2 (Figs. S3–4). Also notable is the fact that the 3'UTR of Nrf2 possesses two possible binding sites for miR-144-3p as opposed to only one binding site for miR-144-5p (Fig. 6A). To confirm the predicted interaction(s) of the 5p and 3p strands of miR-144 with the 3'-UTR of Nrf2, luciferase reporter assays were conducted (Fig. 6B,D). In brief, human RPE cells were transfected with miR-144-5p or miR-144-3p mimics with or without transfection of the 3'-UTR Nrf2 construct. When co-transfected with the 3'UTR of Nrf2, a decrease in relative fluorescence was observed with both miR-144-5p and miR-144-3p indicating that each of the respective strands are indeed capable of interacting with the 3'UTR of Nrf2 as suggested by the *in silico* analyses. Further, using actinomycin-D, a transcriptional inhibitor, we observed that binding of both miR-144-5p and miR-144-3p to 3'-UTR of Nrf2 results in its degradation (Fig. 6C, E). Because the predicted potential binding sites of miR-144-5p and miR-144-3p differ, it is possible that both the 3p and 5p strands could bind the 3'UTR of Nrf2 simultaneously. Although this type of interaction may or may not occur in the *in vivo* condition, we tested this additional potential synergistic method of binding and its impact on the expression of Nrf2, NQO1, GCLC, GSH levels and cell viability in the presence and absence of t-BHP in our experimental system (Fig. S5).

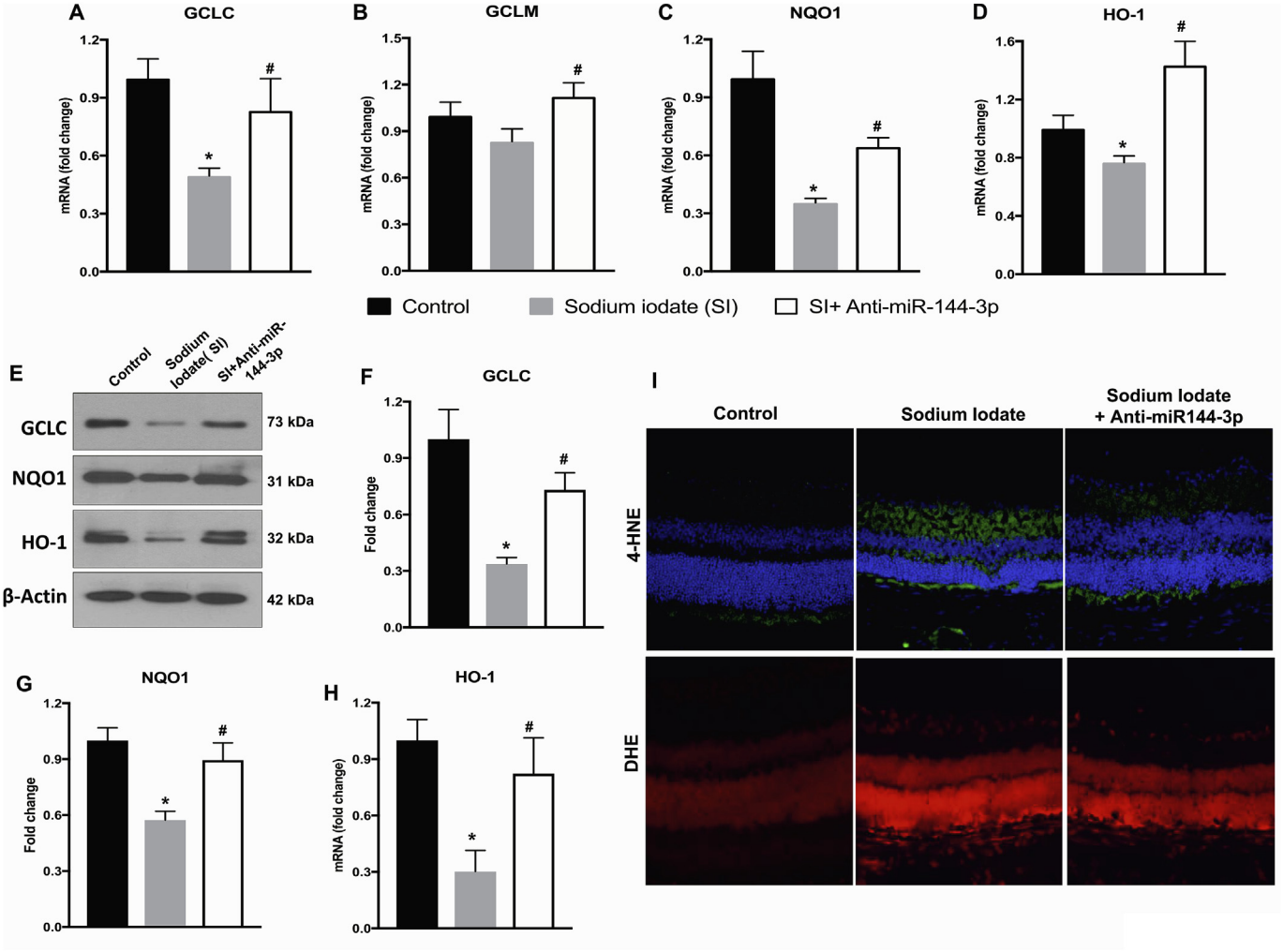

Fig. 8. Effect of miR-144-3p inhibition on oxidative stress and antioxidant signaling in sodium iodate-induced (SI) treated mice.
Eight week old male C57BL/6J mice were treated with PBS (Day 0), 50 mg/kg SI (day 0) once and 50 mg/kg SI (day 0) + 5 μg anti-miR-144-3p (day 1). All animals were sacrificed on day 14 to collect RPE/eye cup for further analysis. **(A)** 4-hydroxynonenol and **(B)** dihydroethidium staining images showing occurrence of oxidative stress in different treatment groups. **(C–F)** mRNA and **(G–J)** protein expression of antioxidant genes was evaluated by qPCR and western blotting respectively. Results are expressed as mean ± S.E.M for n = 6. *p < 0.05 vs. control mice and #p < 0.05 vs. sodium iodate.

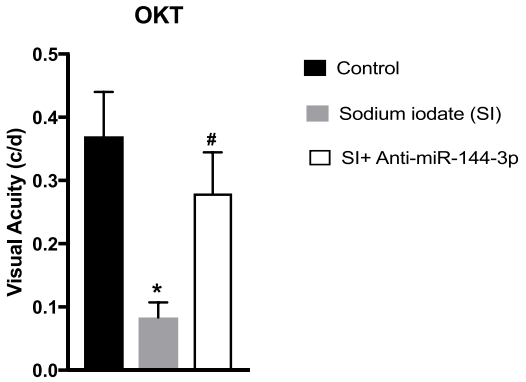

Fig. 9. Effect of miR-144-3p inhibition on visual functions in sodium iodate-induced (SI) treated mice.
Eight week old male C57BL/6J mice were treated with PBS (Day 0), 50 mg/kg SI (day 0) once and 50 mg/kg SI (day 0) + 5 μg anti-miR-144-3p (day 1). All animals were subjected to optokinetic tracking (OKT) testing to evaluate visual function. Results are expressed as mean ± S.E.M for n = 5–6. *p < 0.05 vs. control mice and #p < 0.05 vs. sodium iodate.

3.5. miR-144-3p inhibition protects against retinal degeneration in the sodium iodate mouse model of oxidant-induced outer retinal damage

The above *in vitro* data coupled with literature reports derived from studies of other cell and tissue systems suggest that modulating (suppressing) miR-144 expression may be an effective means of protecting RPE cells from oxidative insult and consequent damage. Therefore, we sought next to determine whether this protection extrapolates to RPE *in vivo*. To this point, our results with miR-144-5p and miR-144-3p have been virtually indistinguishable. However, *in silico* target analyses revealed potentially important differences in these two mature miRs and we know that miR-144-3p is more highly conserved across species. Therefore, going forward to *in vivo* studies, we focused solely on miR-144-3p. We evaluated the impact of miR-144-3p suppression in the sodium iodate mouse model, an established model of pro-oxidant induced outer retinal damage [28-31,46-49]. In brief, sodium iodate (50 mg/kg i.p) was used to induce retinal degeneration; anti-miR-144-3p or vehicle (control) was injected sub-retinally on the following day. This strategy of inhibiting miR-144-3p expression provided considerable protection against sodium iodate-induced outer retinal degeneration as evidenced by significant morphological improvements (e.g., preservation of total retinal thickness) and reduced apoptosis (TUNEL and cleaved caspase-3) in the retina (Figs. 7A and B–C, respectively).

These findings were corroborated by additional detailed morphometric analyses (Fig. 7D–H).

To determine whether the improvements in retinal health observed in association with antagomir-mediated suppression of miR-144-3p (Fig. *S6*) expression coincide with generalized improvements in tissue levels of oxidative stress and/or the expression of Nrf2 and dependent antioxidant response genes, we monitored the expression of several downstream antioxidant target genes (GCLC, GCLM, NQO1, HO-1) as well as 4-hydroxynonenanl (4-HNE) and dihydroethidium (DHE) expression. As per mRNA and protein analyses, Nrf2 signaling was bolstered (Fig. 8A–H) and, oxidative stress was limited (Fig. 8I) in the eyes of sodium-iodate mice treated with miR-144-3p specific antagomir. Importantly, histological and molecular findings demonstrating the protective effects of inhibiting miR-144-3p expression were amply supported by optokinetic tracking studies, which confirmed significant improvements in visual acuity in rodents treated with SI and miR-144-3p antagomir (SI + anti-miR-144-3p; Fig. 9).

4. Discussion

There is an abundance of clinical and experimental evidence that demonstrates emphatically the tremendous threat that unregulated oxidative stress poses to the structural and functional integrity of the RPE. Therefore, efforts to develop therapies that limit the generation of exorbitant levels of oxidative stress within this epithelial cell layer are warranted [4,34]. MiRNAs represent attractive potential targets because these regulatory molecules independently modulate, some positively and some negatively, the expression of hundreds of genes that play key roles in metabolism. Thus, understanding better the roles of miRNAs and their target genes may provide a more comprehensive understanding of mechanisms directly relevant to aging and/or disease development and progression. Of late, a number of oxidative stress responsive miRNAs have been identified and related studies show potential benefit in the above regard in association with their suppressed expression [23,35,36]. This has been evaluated quite heavily in the cancer field and more recently in neurodegenerative disease but interestingly, not abundantly in the context of RPE and/or neuroretina. Given the commonality of oxidant-induced damage to these tissues in the pathogenesis and progression of degenerative retinal disease, bridging this gap in knowledge is important. Therefore, in the present study, we evaluated the relevance of the miR-144, a miR that has been consistently shown to be upregulated in neurodegenerative conditions in which dysregulated antioxidant signaling plays a major causative role [37].

According to the canonical pathway of miRNA biogenesis, miRNA primary transcripts are processed and exported to the cytoplasm where double-stranded duplexes are generated through the action of Dicer in the RNA induced silencing complex (RISC) [38–40]. Two mature miRNA species may be generated from the 5' and 3' arms of a single pre-miRNA precursor and in most cases, only one of these species remains while the complementary species is degraded [38–40]. In recent years however, the co-existence of miRNA-5p and -3p species has been increasingly reported [41,42]. Additionally, it is now well established that the 3p and 5p variants of miRNAs can target either the same [43] or different [44] proteins to regulate disease conditions. Therefore, in the present study, we considered the potential contributions of both miR-144-5p and miR-144-3p to the regulation of oxidative stress responses in RPE. Our initial *in vitro* studies were congruent with the former scenario, both the 5p and 3p miRNAs targeted the 3/UTR of Nrf2 similarly, and the consequent effects on levels of GSH and cell viability were very similar. Our finding that miR-144 expression correlates inversely to the expression and activity of Nrf2 is supported by similar recent findings in other cell and tissue types [25–27] but, interestingly do not agree with a previous report of miR-144 expression in RPE cells exposed to oxidative stress [28]. Key potential differences between our present study and that of Garcia et al [28] that could account for the discrepancy amongst the findings of the two studies are the nature and duration of oxidative stress. Garcia et al. [28] treated cells chronically (3 weeks) and with paraquat. We, on the other hand, exposed RPE cells to hypoxic conditions or to t-BHP and monitored the acute response (0–4 h) of cells to these stimuli. Thus, the decrease in expression of miR-144 observed in the study by Garcia et al. could be the end result of chronic oxidative stress following a prolonged exposure as opposed to the early, rapid response to pro-oxidant insult that we observed. This speculation is supported by our own later *in vivo* findings in the SI mouse model (Fig. S6, blue line) in which we see that miR-144 expression initially increases following SI administration but tapers off with increased time. Further, in the study by Garcia et al. no distinction between the 3p or 5p variant or miR-144 was made.

The findings of our *in vitro* studies were supported further by target prediction analyses performed using TargetScan (www.targetscan.org). These analyses demonstrated that the 3p and 5p variants of miR-144 actually have few common targets however, of the shared targets that exist, Nrf2, a key redox signaling molecule stood out. Others and we have demonstrated the importance of Nrf2 signaling in various forms of retinal degeneration and a number of potential regulatory miRNAs have been proposed [15,18,45–47]. Because our *in vitro* studies were quite promising, we used the sodium iodate model, one of the most consistent and widely used acute models of oxidant-induced RPE damage and outer retinal degeneration [29,48–51], to determine whether the regulatory effects of miR-144 5p and 3p on redox signaling that were observed in cultured human RPE reflect actual redox signaling in RPE *in vivo*. In this subset of studies, we focused on miR-144-3p, a decision based overwhelmingly on information provided by TargetScan analyses. In doing so, we hoped that given that the potential for achieving good *in vivo* benefit with respect to limiting oxidative stress and circumventing potential unwanted side effect might be greater using a single low to moderate dose of 3p antagomir rather than 5p antagomir given the multiple potential binding sites for miR-144-3p in the 3'UTR of Nrf2. Indeed, we found that a single sub-retinal injection of anti-miR-144-3p provided protection against retinal degeneration in the sodium iodate model as indicated by the overall improvement in retinal morphology and visual acuity. Further, analyses of Nrf2, NQO1 and GCLC suggested that the protection conferred by injection of miR-144-3p antagomir was indeed a direct result of enhanced antioxidant responses.

As eluded to previously, the search for regulatory nucleotide sequences that have specific gene targets have put miRNAs at the forefront of studies aimed at identifying biomarkers and/or developing novel therapeutics. Therefore, it is of crucial importance to gain insight into the role of miRNAs both normally and in degenerative diseases of RPE/retina [52,53]. Thus, our *in vivo* studies are particularly important as not only did they corroborate well with our *in vitro* findings demonstrating a key role for miR-144 in the regulation of antioxidant defense regulation under normal conditions but, they additionally provided compelling evidence in support of the potential efficacy of therapies to suppress miR-144-3p to protect against oxidant-induced damage to RPE in conditions relevant to human disease. Indeed, our current work coupled with that of others demonstrating the decline of miR-144 expression in aging and degenerative diseases of brain and retina [37,54] implicate this miR causatively in the reduced efficiency of antioxidant defense mechanisms characteristic of these conditions. Our work additionally provides novel insight into the role of miR-144 in regulating Nrf2-dependent redox signaling in RPE. Future exploration of the influence of redox sensitive miRNA-induced epigenetic control of the Nrf2 signaling pathway and its cross talk, particularly in RPE, could provide insight into therapeutic options for retinal degenerative diseases involving this cell type. As such, detailed follow-up studies are warranted to determine whether focal administration of inhibitors of miR-144 could be employed therapeutically to prevent, slow or treat the development of outer retinal pathology characteristic of aging (e.g., age-related macular degeneration) and/or disease (e.g., diabetic

retinopathy). Such studies are broadly relevant clinically.

Declaration of competing interest

The authors have no conflicts to declare.

Acknowledgements

We would like to thank Jianghe Yuan for assistance with animal studies. We would additionally like to acknowledge funding support for these studies from National Eye Institute grants EY022704 and EY029113 to Pamela Martin and grant EY022416 to Manuela Bartoli and, Augusta University Research Institute grant IGPB00002 to Pamela Martin.

Appendix A. Supplementary data

Supplementary data to this article can be found online at https://doi.org/10.1016/j.redox.2019.101336.

References

[1] R. Simo, M. Villarroel, L. Corraliza, C. Hernandez, M. Garcia-Ramirez, The retinal pigment epithelium: something more than a constituent of the blood-retinal barrier–implications for the pathogenesis of diabetic retinopathy, J. Biomed. Biotechnol. 2010 (2010) 190724.
[2] O. Strauss, The retinal pigment epithelium in visual function, Physiol. Rev. 85 (3) (2005) 845–881.
[3] Y. He, J. Ge, J.M. Burke, R.L. Myers, Z.Z. Dong, J. Tombran-Tink, Mitochondria impairment correlates with increased sensitivity of aging RPE cells to oxidative stress, J Ocul Biol Dis Infor 3 (3) (2010) 92–108.
[4] S.M. Plafker, G.B. O'Mealey, L.I. Szweda, Mechanisms for countering oxidative stress and damage in retinal pigment epithelium, Int Rev Cell Mol Biol 298 (2012) 135–177.
[5] J.R. Sparrow, D. Hicks, C.P. Hamel, The retinal pigment epithelium in health and disease, Curr. Mol. Med. 10 (9) (2010) 802–823.
[6] S.M. Cohen, K.L. Olin, W.J. Feuer, L. Hjelmeland, C.L. Keen, L.S. Morse, Low glutathione reductase and peroxidase activity in age-related macular degeneration, Br. J. Ophthalmol. 78 (10) (1994) 791–794.
[7] P.S. Samiec, C. Drews-Botsch, E.W. Flagg, J.C. Kurtz, P. Sternberg Jr., R.L. Reed, D.P. Jones, Glutathione in human plasma: decline in association with aging, age-related macular degeneration, and diabetes, Free Radic. Biol. Med. 24 (5) (1998) 699–704.
[8] M. Nita, A. Grzybowski, The role of the reactive oxygen species and oxidative stress in the pathomechanism of the age-related ocular diseases and other pathologies of the anterior and posterior eye segments in adults, Oxid Med Cell Longev 2016 (2016) 3164734.
[9] N. Golestaneh, Y. Chu, Y.Y. Xiao, G.L. Stoleru, A.C. Theos, Dysfunctional autophagy in RPE, a contributing factor in age-related macular degeneration, Cell Death Dis. 8 (1) (2017) e2537.
[10] S. Guha, J. Liu, G. Baltazar, A.M. Laties, C.H. Mitchell, Rescue of compromised lysosomes enhances degradation of photoreceptor outer segments and reduces lipofuscin-like autofluorescence in retinal pigmented epithelial cells, Adv. Exp. Med. Biol. 801 (2014) 105–111.
[11] M.L. Lambros, S.M. Plafker, Oxidative stress and the Nrf2 anti-oxidant transcription factor in age-related macular degeneration, Adv. Exp. Med. Biol. 854 (2016) 67–72.
[12] B.S. Winkler, M.E. Boulton, J.D. Gottsch, P. Sternberg, Oxidative damage and age-related macular degeneration, Mol. Vis. 5 (1999) 32.
[13] Q. Ma, Role of nrf2 in oxidative stress and toxicity, Annu. Rev. Pharmacol. Toxicol. 53 (2013) 401–426.
[14] A. Raghunath, K. Sundarraj, R. Nagarajan, F. Arfuso, J. Bian, A.P. Kumar, G. Sethi, E. Perumal, Antioxidant response elements: discovery, classes, regulation and potential applications, Redox Biol 17 (2018) 297–314.
[15] Y. Nakagami, Nrf2 is an attractive therapeutic target for retinal diseases, Oxid Med Cell Longev 2016 (2016) 7469326.
[16] H. Cho, M.J. Hartsock, Z. Xu, M. He, E.J. Duh, Monomethyl fumarate promotes Nrf2-dependent neuroprotection in retinal ischemia-reperfusion, J. Neuroinflammation 12 (2015) 239.
[17] H. Pan, M. He, R. Liu, N.C. Brecha, A.C. Yu, M. Pu, Sulforaphane protects rodent retinas against ischemia-reperfusion injury through the activation of the Nrf2/HO-1 antioxidant pathway, PLoS One 9 (12) (2014) e114186.
[18] W. Promsote, F.L. Powell, S. Veean, M. Thounaojam, S. Markand, A. Saul, D. Gutsaeva, M. Bartoli, S.B. Smith, V. Ganapathy, P.M. Martin, Oral monomethyl fumarate therapy ameliorates retinopathy in a humanized mouse model of sickle cell disease, Antioxidants Redox Signal. 25 (17) (2016) 921–935.
[19] A. Silva-Palacios, M. Ostolga-Chavarria, C. Zazueta, M. Konigsberg, Nrf2: molecular and epigenetic regulation during aging, Ageing Res. Rev. 47 (2018) 31–40.
[20] C. Zhou, L. Zhao, J. Zheng, K. Wang, H. Deng, P. Liu, L. Chen, H. Mu, MicroRNA-144 modulates oxidative stress tolerance in SH-SY5Y cells by regulating nuclear factor erythroid 2-related factor 2-glutathione axis, Neurosci. Lett. 655 (2017) 21–27.
[21] K. Felekkis, E. Touvana, C. Stefanou, C. Deltas, microRNAs: a newly described class of encoded molecules that play a role in health and disease, Hippokratia 14 (4) (2010) 236–240.
[22] Y. Wan, R. Cui, J. Gu, X. Zhang, X. Xiang, C. Liu, K. Qu, T. Lin, Identification of four oxidative stress-responsive MicroRNAs, mir-34a-5p, mir-1915-3p, mir-638, and mir-150-3p, in hepatocellular carcinoma, Oxid Med Cell Longev 2017 (2017) 5189138.
[23] J. Banerjee, S. Khanna, A. Bhattacharya, MicroRNA regulation of oxidative stress, Oxid Med Cell Longev 2017 (2017) 2872156.
[24] H. Yaribeygi, S.L. Atkin, A. Sahebkar, Potential roles of microRNAs in redox state: an update, J. Cell. Biochem. (2018), https://doi.org/10.1002/jcb.27475 In press.
[25] A.T. Kukoyi, X. Fan, B.S. Staitieh, B.M. Hybertson, B. Gao, J.M. McCord, D.M. Guidot, MiR-144 mediates Nrf2 inhibition and alveolar epithelial dysfunction in HIV-1 transgenic rats, Am. J. Physiol. Cell Physiol. 317 (2) (2019) C390–C397, https://doi.org/10.1152/ajpcell.00038.2019.
[26] B. Li, X. Zhu, C.M. Ward, A. Starlard-Davenport, M. Takezaki, A. Berry, A. Ward, C. Wilder, C. Neunert, A. Kutlar, B.S. Pace, MIR-144-mediated NRF2 gene silencing inhibits fetal hemoglobin expression in sickle cell disease, Exp. Hematol. 70 (2019) 85–96 e5.
[27] S. Zhou, W. Ye, Y. Zhang, D. Yu, Q. Shao, J. Liang, M. Zhang, miR-144 reverses chemoresistance of hepatocellular carcinoma cell lines by targeting Nrf2-dependent antioxidant pathway, Am. J. Tourism Res. 8 (7) (2016) 2992–3002.
[28] T.Y. Garcia, M. Gutierrez, J. Reynolds, D.A. Lamba, Modeling the dynamic AMD-associated chronic oxidative stress changes in human ESC and iPSC-derived RPE cells, Investig. Ophthalmol. Vis. Sci. 56 (12) (2015) 7480–7488.
[29] G. Chowers, M. Cohen, D. Marks-Ohana, S. Stika, A. Eijzenberg, E. Banin, A. Obolensky, Course of sodium iodate-induced retinal degeneration in albino and pigmented mice, Investig. Ophthalmol. Vis. Sci. 58 (4) (2017) 2239–2249.
[30] A.E. Koh, H.A. Alsaeedi, M.B.A. Rashid, C. Lam, M.H.N. Harun, M. Saleh, C.D. Luu, S.S. Kumar, M.H. Ng, H.M. Isa, S.N. Leow, K.Y. Then, M.C. Bastion, M.S. Ali Khan, P.L. Mok, Retinal degeneration rat model: a study on the structural and functional changes in the retina following injection of sodium iodate, J. Photochem. Photobiol. B Biol. 196 (2019) 111514.
[31] M. Moriguchi, S. Nakamura, Y. Inoue, A. Nishinaka, M. Nakamura, M. Shimazawa, H. Hara, Irreversible photoreceptors and RPE cells damage by intravenous sodium iodate in mice is related to macrophage accumulation, Investig. Ophthalmol. Vis. Sci. 59 (8) (2018) 3476–3487.
[32] Q. Nie, X. Gong, L. Gong, L. Zhang, X. Tang, L. Wang, F. Liu, J.L. Fu, J.W. Xiang, Y. Xiao, Z. Luo, R. Qi, Z. Chen, Y. Liu, Q. Sun, W. Qing, L. Yang, J. Xie, M. Zou, Y. Gan, H. Chen, D.W. Li, Sodium iodate-induced mouse model of age-related macular degeneration displayed altered expression patterns of sumoylation enzymes E1, E2 and E3, Curr. Mol. Med. 18 (8) (2018) 550–555.
[33] G.T. Prusky, N.M. Alam, S. Beekman, R.M. Douglas, Rapid quantification of adult and developing mouse spatial vision using a virtual optomotor system, Investig. Ophthalmol. Vis. Sci. 45 (12) (2004) 4611–4616.
[34] S.G. Jarrett, M.E. Boulton, Consequences of oxidative stress in age-related macular degeneration, Mol. Asp. Med. 33 (4) (2012) 399–417.
[35] H. Bu, S. Wedel, M. Cavinato, P. Jansen-Durr, MicroRNA regulation of oxidative stress-induced cellular senescence, Oxid Med Cell Longev 2017 (2017) 2398696.
[36] A. Magenta, S. Greco, C. Gaetano, F. Martelli, Oxidative stress and microRNAs in vascular diseases, Int. J. Mol. Sci. 14 (9) (2013) 17319–17346.
[37] S.P. Persengiev, Kondova II, R.E. Bontrop, The impact of MicroRNAs on brain aging and neurodegeneration, Curr Gerontol Geriatr Res 2012 (2012) 359369.
[38] J. O'Brien, H. Hayder, Y. Zayed, C. Peng, Overview of MicroRNA biogenesis, mechanisms of actions, and circulation, Front Endocrinol (Lausanne) 9 (2018) 402.
[39] S.K. Pong, M. Gullerova, Noncanonical functions of microRNA pathway enzymes - drosha, DGCR8, Dicer and Ago proteins, FEBS Lett. 592 (17) (2018) 2973–2986.
[40] K. Saliminejad, H.R. Khorram Khorshid, S. Soleymani Fard, S.H. Ghaffari, An overview of microRNAs: biology, functions, therapeutics, and analysis methods, J. Cell. Physiol. 234 (5) (2018) 5451–5465, https://doi.org/10.1002/jcp.27486.
[41] S. Griffiths-Jones, J.H. Hui, A. Marco, M. Ronshaugen, MicroRNA evolution by arm switching, EMBO Rep. 12 (2) (2011) 172–177.
[42] J.S. Yang, M.D. Phillips, D. Betel, P. Mu, A. Ventura, A.C. Siepel, K.C. Chen, E.C. Lai, Widespread regulatory activity of vertebrate microRNA* species, RNA 17 (2) (2011) 312–326.
[43] C.J. Huang, P.N. Nguyen, K.B. Choo, S. Sugii, K. Wee, S.K. Cheong, T. Kamarul, Frequent co-expression of miRNA-5p and -3p species and cross-targeting in induced pluripotent stem cells, Int. J. Med. Sci. 11 (8) (2014) 824–833.
[44] X. Yang, W.W. Du, H. Li, F. Liu, A. Khorshidi, Z.J. Rutnam, B.B. Yang, Both mature miR-17-5p and passenger strand miR-17-3p target TIMP3 and induce prostate tumor growth and invasion, Nucleic Acids Res. 41 (21) (2013) 9688–9704.
[45] S. Batliwala, C. Xavier, Y. Liu, H. Wu, I.H. Pang, Involvement of Nrf2 in ocular diseases, Oxid Med Cell Longev 2017 (2017) 1703810.
[46] X.F. Liu, D.D. Zhou, T. Xie, J.L. Hao, T.H. Malik, C.B. Lu, J. Qi, O.P. Pant, C.W. Lu, The Nrf2 signaling in retinal ganglion cells under oxidative stress in ocular neurodegenerative diseases, Int. J. Biol. Sci. 14 (9) (2018) 1090–1098.
[47] F. Lamoke, S. Shaw, J. Yuan, S. Ananth, M. Duncan, P. Martin, M. Bartoli, Increased oxidative and nitrative stress accelerates aging of the retinal vasculature in the diabetic retina, PLoS One 10 (10) (2015) e0139664.
[48] C. Chen, M. Cano, J.J. Wang, J. Li, C. Huang, Q. Yu, T.P. Herbert, J.T. Handa, S.X. Zhang, Role of unfolded protein response dysregulation in oxidative injury of retinal pigment epithelial cells, Antioxidants Redox Signal. 20 (14) (2014) 2091–2106.
[49] R. Kannan, D.R. Hinton, Sodium iodate induced retinal degeneration: new insights

from an old model, Neural Regen Res 9 (23) (2014) 2044–2045.
[50] A. Baich, J. Schloz, The formation of glyoxylate from glycine by melanin, Biochem. Biophys. Res. Commun. 159 (3) (1989) 1161–1164.
[51] A. Baich, M. Ziegler, The effect of sodium iodate and melanin on the formation of glyoxylate, Pigment Cell Res. 5 (6) (1992) 394–395.
[52] P. Berber, F. Grassmann, C. Kiel, B.H. Weber, An eye on age-related macular degeneration: the role of MicroRNAs in disease pathology, Mol. Diagn. Ther. 21 (1) (2017) 31–43.
[53] A. Raghunath, E. Perumal, Micro-RNAs and their roles in eye disorders, Ophthalmic Res. 53 (4) (2015) 169–186.
[54] J.H. Wu, Y. Gao, A.J. Ren, S.H. Zhao, M. Zhong, Y.J. Peng, W. Shen, M. Jing, L. Liu, Altered microRNA expression profiles in retinas with diabetic retinopathy, Ophthalmic Res. 47 (4) (2012) 195–201.